JMEPEG (2009) 18:1264–1271
DOI: 10.1007/s11665-009-9378-x

1059-9495/$19.00

Corrosion Mechanism of Low-Carbon Steel in Industrial Water and Adsorption Thermodynamics in the Presence of Some Plant Extracts

A.M. Badiea and K.N. Mohana

(Submitted May 14, 2008; in revised form January 17, 2009)

The effects of radish leaves and black cumin as plant extracts on the corrosion behavior of low-carbon steel in industrial water in the temperature range of 30 to 80 °C and velocity range of 1.44 to 2.02 m s^{-1} using potentiodynamic polarization, electrochemical impedance spectroscopy, and mass loss measurements have been investigated. The inhibition efficiency increased with increasing concentration of the plant extracts up to a critical value but it slightly decreased with increasing temperature. Inhibition efficiency values obtained from mass loss and potentiodynamic data were in reasonable agreement. Potentiodynamic polarization clearly indicated that radish leaves and black cumin extracts acted as anodic inhibitors. The adsorption behavior was found to obey the Flory-Huggins isotherm model. The associated activation parameters and thermodynamic data of adsorption were evaluated and discussed. The results show that radish leaves and black cumin could serve as effective inhibitors for low-carbon steel in industrial water media, with black cumin providing better protection than radish leaves.

Keywords corrosion, metals and alloys, polarization, surfaces and interfaces

1. Introduction

Nowadays, natural compounds from herb plants are being used as corrosion inhibitors to develop new clean chemicals for green environment. Herb plants which usually are used as herbal medicine have been selected because they are environmentally acceptable, readily available, and renewable. Plant extracts are viewed as an incredibly rich source of naturally synthesized chemical compounds that can be extracted by simple extract procedures with low cost (Ref 1). Relatively few investigations have been reported using such economic plant extract. Saleh et al. (Ref 2) reported that Opunia extract, Aleo eru leaves, orange, and mango peels give adequate protection to steel in 5% and 10% HCl at 25 and 40 °C. Srivatsava and Srivatsava (Ref 3) found that tobacco, black pepper, caster oil seeds, acacia gum, and lignin can be good inhibitors for steel in acidic medium. El-Etre (Ref 4, 5) studied the application of natural honey as corrosion inhibitor for carbon steel and copper in aqueous solution. Khamis and Al-Andis (Ref 6) proved the use of herbs such as coriander, hibiscus, anis, black cumin, and garden cress as new inhibitors for acidic corrosion of steel. Black cumin also was studied by Abdel-Gaber et al. (Ref 1) as inhibitor for carbon steel in acidic medium. The application of extracts of henna, thyme, bgugaine, and inriine was investigated for their anticorrosion activity (Ref 7-9).

This article reports the results of an investigation on inhibitive performance of radish leaves and black cumin on low-carbon steel at various velocities and temperatures of industrial water using electrochemical impedance spectroscopy (EIS) and potentiodynamic polarization technique. Additionally, the adsorption behavior of radish leaves and black cumin on low-carbon steel in industrial water was studied.

A.M. Badiea and **K.N. Mohana**, Department of Chemistry, University of Mysore, Manasagangotri, Mysore 570 006, India. Contact e-mail: badeea7@yahoo.com.

2. Experimental Work

2.1 Materials Preparation

The specimens used for corrosion tests were cut from low-carbon steel pipes which have the following composition (wt.%): 0.15 C; 0.37 Si; 0.04 P; 0.01 Al; 0.05 Mn; 0.05 S, and the remainder iron. The dimensions of the specimen are 19.2 mm diameter, 5 mm thickness, and 5 mm length. The test solution used was industrial water coming from heat exchangers and reboilers of the chemical industries in and around Mysore city, India. The pH of the industrial water was 6.9 and the chemical composition (ppm) using ionic chromatograph was: 65156 Cl^-; 950 Ca^{2+}; 650SO_4^{2-}; 450 Mg^{2+}; 61HCO_3^-; and 18654 Na^+. Prior to gravimetric and electrochemical measurements, the surface of the specimens was polished under running tap water using emery paper SiC (grade 220-600), rinsed with distilled water, dried on a clean tissue paper, immersed in benzene for 5 s, dried and immersed in acetone for 5 s, and dried with clean tissue paper. Finally, the specimens were kept in a desiccator until use. At the end of the test, the specimens were carefully washed with acetone and benzene, dried, and then weighed.

2.2 Solution Preparation

Double distilled water and analytical reagent grade H_2SO_4 were used for preparing solutions. Stock solution of plant extracts was obtained by drying the plant for 2 h in an oven at 80 °C and grinding it to orderly form. A 10 g sample of the powder was refluxed in 100 mL double distilled water for one day. The refluxed water was filtered to remove any contamination. The concentration of the stock solution was determined by evaporating 10 mL of the filtrate and weighing the residue. Prior to each experiment, 4 M H_2SO_4 was added to an appropriate volume of the stock solution and double distilled water to obtain a solution of 1 M H_2SO_4 and the required concentration of the extract.

2.3 Method

2.3.1 Mass Loss Measurements. Gravimetric experiments were carried out in a round glass cell with three nicks. The solution volume was 400 mL. The initial weight of the specimen was recorded using an analytical balance (precision ±0.1 mg) before immersion in the industrial water. Temperature of the solution was maintained by thermostatically controlled water bath (Eltek Ltd., Mumbai, India). The velocity of the specimens was set at a desired speed using speed regulator motor (Weiber Ltd., Chennai, India).

The corrosion rate (CR) of low-carbon steel has been determined for 10 h of immersion period at various rotational speeds (1500 to 2100 rpm) at temperature range of 30 to 80 °C in aerated solutions from mass loss method using Eq 1, where W is the mass loss (g), A is the area of the coupon (mm^2), ρ is the density of low-carbon steel (g cm^{-3}), and t is the immersion time (h). The CR is expressed in mpy. The experiments were done in triplicate and the average value of the mass loss was reported.

$$\mathrm{CR} = \frac{344.88 \times 10^6 W}{\rho A t} \qquad \text{(Eq 1)}$$

2.3.2 Electrochemical Measurements (EIS). The classical three-electrode configuration was used. An anodized sample as working electrode with an exposed area of 302 mm^2, a saturated calomel electrode as reference electrode, and a platinum sheet as auxiliary electrode were employed. The test solution was industrial water and the electrochemical cell was kept in a room, open to air. Impedance tests were realized 2 days after anodizing/sealing. EIS tests have been conducted at open-circuit conditions using a Solartron Frequency Response Analyser (FRA) Model 1260 and an electrochemical interface, potentiostat Solartron 1286, including a personal computer with CorrWare software, and the electrochemical cell.

Electrochemical impedance spectroscopy tests were in the frequency range of 1000 Hz to 10 MHz with applied potential signal of 10 mV around the open potential. The potentiodynamic polarization experiments were carried out by means of potentiostat regulation using a solartron 1286 electrochemical interface. A cylindrical low-carbon steel rod, saturated calomel electrode (SCE, +242 mV versus SHE), and platinum wire were used as the working, reference, and counter electrode, respectively. The EIS and polarization curves have been performed in aerated solution of industrial water under various concentrations of plant extracts, various rotational speeds, and at different temperatures of environment. Before recording the polarization and EIS curves, the open-circuit potential was stable within 30 min. In the polarization, the cathodic branches were always determined first; the open-circuit potential was then reestablished and the anodic branches were determined. The anodic and cathodic polarization curves were recorded by constant sweep rate of 0.42 mV s^{-1}. The CR from interaction of the Tafel slopes in polarization curves can be calculated from the following equation:

$$\mathrm{CR} = \frac{0.1287 \times I_{\mathrm{corr}} \times \mathrm{eq.wt}}{\rho} \qquad \text{(Eq 2)}$$

where I_{corr} is the corrosion current density (μA cm^{-2}), eq.wt is the equivalent weight of low-carbon steel (g), and ρ is the density of low-carbon steel (g cm^{-3}).

3. Results and Discussions

3.1 Effect of Temperature

The effects of temperature range of 30 to 80 °C on the corrosion current density of low-carbon steel in industrial water at various concentrations of black cumin and radish leaves at different flow velocities of the solution have been studied using potentiodynamic polarization and gravimetric measurements. The inhibition efficiency of the plant extracts from mass loss, polarization, and EIS methods can be calculated as follows:

$$\mathrm{IE}\ (\%) = \left(1 - \frac{X_{(\mathrm{p})}}{X_{(\mathrm{a})}}\right) \times 100 \qquad \text{(Eq 3)}$$

where X is CR or I_{corr}, or $1/R_{\mathrm{ct}}$ (R_{ct} is the charge transfer resistance) and the subscript p and a indicate presence and absence of the inhibitors, respectively.

The results obtained from gravimetric method after 10 h immersion for low-carbon steel in industrial water in the absence and presence of various concentrations of black cumin and radish leaves extracts at 30 °C and at 1.44 and 1.56 m s^{-1} velocity are depicted in Table 1. These results show that both the tested plant extracts inhibit the corrosion of low-carbon steel in industrial water at all concentrations used in this study.

The values of corrosion current density (I_{corr}), corrosion potential (E_{corr}) and IE (%) at 1.44 and 1.56 m s^{-1} and at 30 °C are tabulated in Table 2. Table 2 shows that the values of E_{corr}

Table 1 Corrosion rate of low-carbon steel and inhibition efficiency of inhibitors for various concentrations of radish leaves and black cumin in industrial water at 30 °C and at 1.44 and 1.56 m s^{-1} obtained from mass loss measurements

		1.44 m s^{-1}		1.56 m s^{-1}	
Plant	C, g L^{-1}	CR, mpy	IE, %	CR, mpy	IE, %
	Blank	14.59	···	16.12	···
Radish leaves	1.20	10.49	28.11	8.51	47.18
	2.00	8.60	41.04	7.24	55.08
	2.50	6.45	55.78	5.78	64.14
	3.88	5.09	65.12	4.55	71.79
Black cumin	0.40	10.12	30.67	7.77	51.78
	0.80	7.45	48.97	6.54	59.45
	1.20	5.42	62.88	4.86	69.86
	1.50	3.83	73.75	4.00	75.17

are shifted toward more positive by increasing the concentrations. Figure 1 shows that the inhibition efficiency of the studied inhibitors at optimal conditions slightly decreased with increasing temperature. This may be attributed to the weakening of the bonds between the metal surface and molecules of plant extracts with increasing temperature. However, the corrosion current density clearly increases with increasing temperature in the absence of inhibitors except at 80 °C. This is because of the escape of oxygen from the open system. But there was a slight increase of I_{corr} in the presence of plant extracts. Figure 2 shows the corrosion current density and corrosion potential relationship for low-carbon steel in industrial water at different temperatures of solution in the presence of 3.88 g L^{-1} radish leaves extracts at 1.56 m s^{-1}. As the temperature increased, the interaction of anodic and cathodic Tafel slopes increased indicating a significant shift toward more logarithmic corrosion current density except at 80 °C. At this temperature, oxygen and solubility of other gases decrease due to the open system. However, when the concentration of radish leaves at 30 °C and at 1.56 m s^{-1} velocity was increased, the interaction of anodic and cathodic Tafel lines decreased, indicating a significant shift toward less logarithmic corrosion current density (Fig. 3). This means that the corrosion current density decreased with increasing concentration. Figure 4 shows the potentiodynamic polarization curves for low-carbon steel in industrial water at optimal conditions in the absence and presence of 1.50 g L^{-1} black cumin and 3.88 g L^{-1} radish

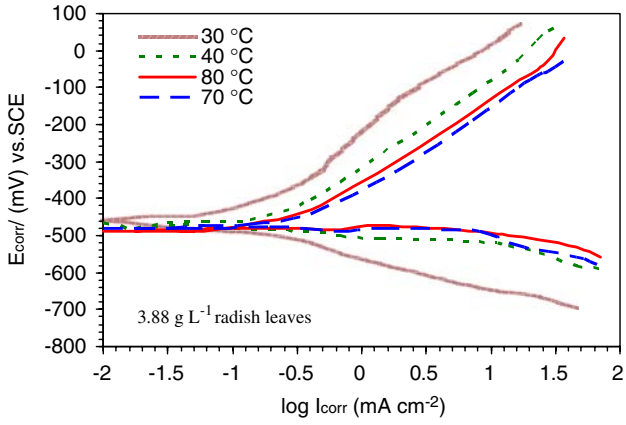

Fig. 2 Potentiodynamic polarization curves for low-carbon steel in industrial water at different temperatures in the presence of 3.88 g L^{-1} radish leaves at 1.56 m s^{-1}

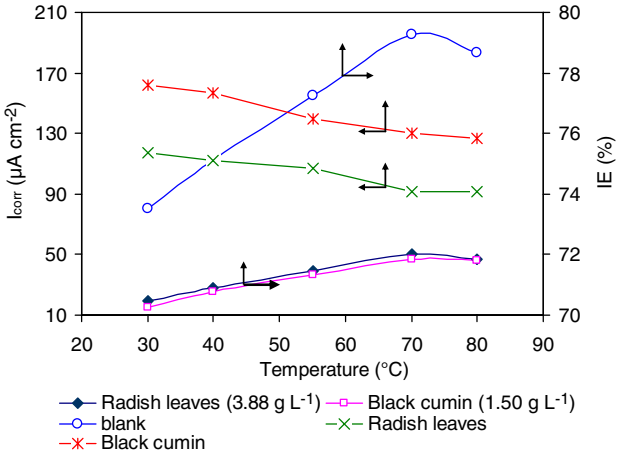

Fig. 1 Effect of temperature on the inhibition efficiency of inhibitors and corrosion current density in the presence and absence of optimum radish leaves and black cumin extracts at 1.56 m s^{-1}

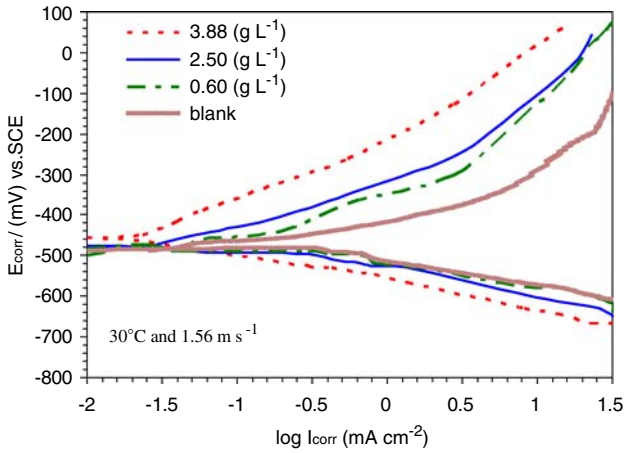

Fig. 3 Potentiodynamic polarization curves for low-carbon steel in industrial water in the presence of different radish leaves extracts concentrations at 30 °C and at 1.56 m s^{-1}

Table 2 Electrochemical parameters for low-carbon steel in industrial water containing different plant extract concentrations at 30 °C and at 1.44 and 1.56 m s^{-1}

		1.44 m s^{-1}			1.56 m s^{-1}		
Plant	***C*, g L^{-1}**	**E_{corr} vs. SCE, mV**	**I_{corr}, µA cm^{-2}**	**IE, %**	**E_{corr} vs. SCE, mV**	**I_{corr}, µA cm^{-2}**	**IE, %**
	Blank	−501	62.50	...	−502	80.35	...
Radish leaves	0.60	−498	54.92	12.12	−500	50.73	36.86
	0.90	−498	50.96	18.46	−489	46.15	42.57
	1.20	−490	43.67	30.13	−483	38.74	51.78
	2.00	−486	35.34	43.46	−480	32.19	59.94
	2.50	−479	27.90	55.37	−476	24.92	68.99
	3.88	−466	20.46	67.26	−461	19.78	75.38
Black cumin	0.15	−496	52.84	15.46	−496	42.76	42.05
	0.40	−488	40.69	34.89	−478	37.85	52.90
	0.80	−481	32.10	48.63	−473	28.48	64.56
	1.20	−468	22.00	64.80	−468	21.75	72.93
	1.50	−464	16.53	73.59	−456	18.01	77.59

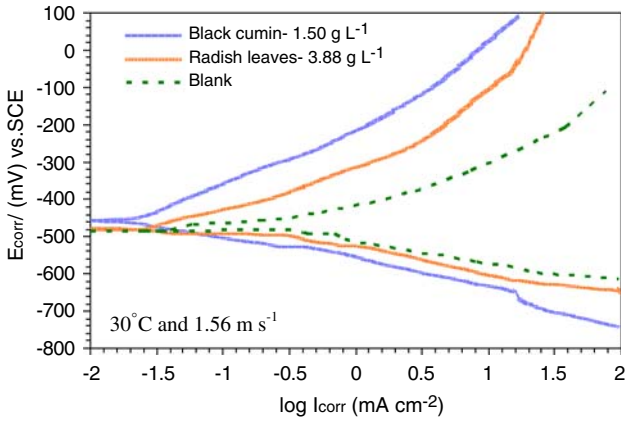

Fig. 4 Potentiodynamic polarization curves for low-carbon steel in industrial water in the absence and presence of optimal concentration of black cumin and radish leaves at 30 °C and at 1.56 m s^{-1}

leaves at 30 °C and at 1.56 m s^{-1}. The anodic and cathodic parts of polarization curves of these two plant extracts indicate that the inhibition action of black cumin is better than radish leaves extracts. It is shown in the polarization curves that the studied plants acted as anodic inhibitors.

In general, for acid solutions, when dissolved oxygen is present, both hydrogen evolution and oxygen reduction reactions will be possible. However, solubility of oxygen in pure water at 25 °C is only about 10^{-3} mol dm^{-3} (Ref 10) and decreases slightly with concentration of dissolved salts. In addition, the concentration of H_3O^+ in acid solutions, at pH ≈ 0, is high, and since this ion has a high rate of diffusion, the contribution made by the hydrogen evolution reaction on the cathodic process will be predominant. Similar observations were recorded for other plant extracts.

Further information on the influence of mechanism of the corrosion of low-carbon steel in industrial water was obtained by calculating the activation energies (E_a) for the corrosion process using the Arrhenius equation,

$$I_{corr} = k \exp\left(\frac{-E_a}{RT}\right) \quad \text{(Eq 4)}$$

where E_a is the activation energy, k is the pre-exponential factor, R is the universal gas constant, and T is the absolute temperature. The Arrhenius plots for the CR of low-carbon steel in industrial water at various concentrations of plant extracts and at 1.56 m s^{-1} velocity are shown in Fig. 5(a) and (b). The values of E_a and k could be obtained from the slopes and intercepts, respectively, of plots of ln CR versus $1/T$. The activation entropy (ΔS_a) and activation enthalpy (ΔH_a) can also be determined from the following equation:

$$I_{corr} = \frac{RT}{Nh} \exp\left(\frac{\Delta S_a}{R}\right) \cdot \exp\left(\frac{-\Delta H_a}{RT}\right) \quad \text{(Eq 5)}$$

where N is the average Avogadro's number and h is the Planck's constant. Plots of ln (I_{corr}/T) versus ($1/T$) gave straight lines with a slope of ($-\Delta H_a/R$) and an intercept of [ln (R/Nh) + $\Delta S_a/R$] as shown in Fig. 6(a) and (b). The values of activation parameters are tabulated in Table 3. The data clearly show that the values of E_a increased with increasing concentration of plant extracts; however, the values of pre-exponential factor (k) decreased. This is the typical state of Arrhenius equation that the higher E_a and the lower k lead to

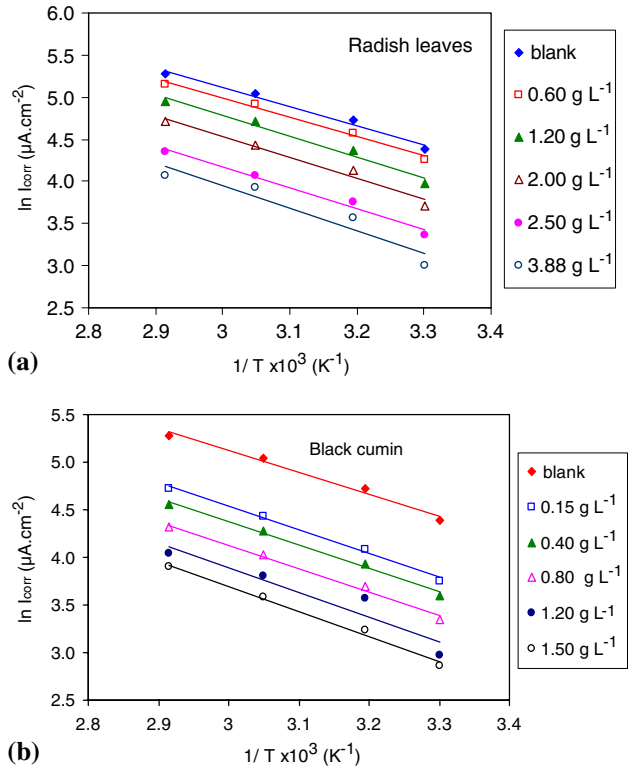

Fig. 5 Arrhenius plots of the CR of low-carbon steel in industrial water in the absence and presence of various concentrations of radish leaves (a) and black cumin (b) extracts at 1.56 m s^{-1}

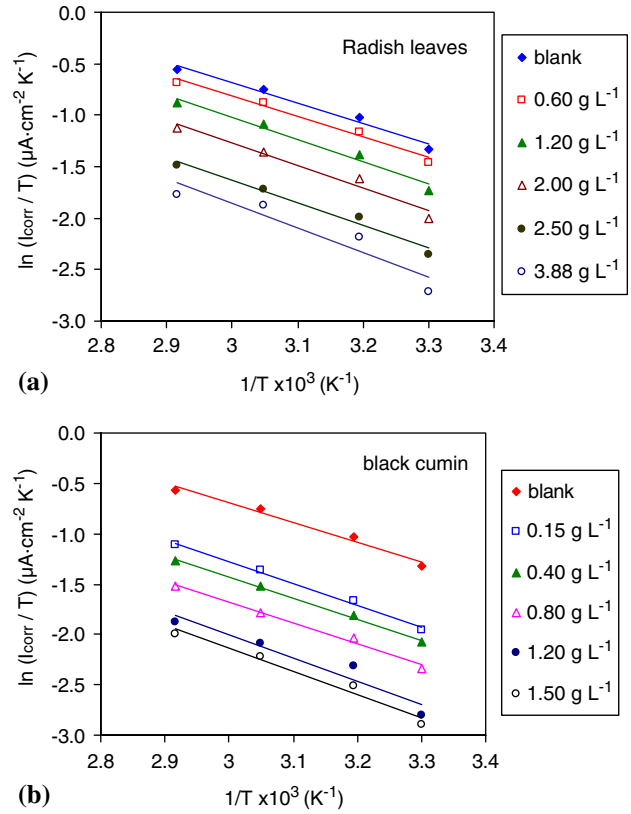

Fig. 6 Eyring plots of the CR of low-carbon steel in industrial water in the absence and presence of various concentrations of radish leaves (a) and black cumin (b) extracts at 1.56 m s^{-1}

the reduction of CR according to Eq 4. This relative increase in E_a due to increase of inhibition efficiency suggests that the rate of formation of the adsorbed film is higher than its rate of destruction and the dissolution of low-carbon steel does not take place on the metal surface.

The positive values of ΔH_a indicate that the dissolution reaction is an endothermic process and that the dissolution of low-carbon steel in industrial water is difficult (Ref 11). The higher values of ΔH_a than those obtained for the uninhibited solution indicate higher protection efficiency. This may be attributed to the presence of an energy barrier for the reaction, that is, the process of adsorption leads to a rise in the enthalpy of the corrosion process (Ref 12). The values of ΔH_a could also be obtained from the following equation:

$$\Delta H_a = E_a - RT \quad \text{(Eq 6)}$$

The values of ΔH_a obtained here are in very good agreement with those obtained from Eq 5, confirming the endothermic process of low-carbon steel dissolution in industrial water. The negative value of ΔS_a implies that the activated complex represents an association rather than a dissociation step, meaning that a decrease in disordering takes place from reactants to the activated complex (Ref 10, 13). Furthermore, the entropy ΔS_a increased negatively in the presence of plant extracts reflecting that the formation of an ordered stable layer of inhibitors on the low-carbon steel in industrial water is possible. As a result of this, the studied inhibitors can be effective inhibitors.

3.2 Electrochemical Impedance Spectroscopy

The results of the potentiodynamic polarization experiments were confirmed by impedance measurements, since the EIS is a powerful technique in studying corrosion mechanisms and adsorption phenomena (Ref 14). The corrosion behavior of low-carbon steel in industrial water in the absence and presence of black cumin extracts was investigated by the EIS technique at 30 °C and 1.56 m s^{-1} after 10 h immersion time and the results are presented by Nyquist plots as shown in Fig. 7. The Nyquist plots are analyzed in terms of the equivalent circuit comprised with classic parallel capacitor and resistor, which contains the solution resistance R_s and the C_{dl} which is placed in parallel to R_{ct} (shown in Fig. 8) (Ref 15, 16). The fitted values of R_{ct}, C_{dl}, and IE (%) are listed in Table 4.

It is found that as the concentration of black cumin increases, R_{ct} values increase (radius of semicircle increases); however, the (C_{dl}) values tend to decrease. The increase of R_{ct} and decrease of C_{dl} values are due to the adsorption of black cumin molecules on the metal surface. The impedance spectra plots were analyzed using a simple equivalent circuit model (Fig. 8). The R_{ct} value is a measure of electron transfer across the surface and inversely proportional to CR.

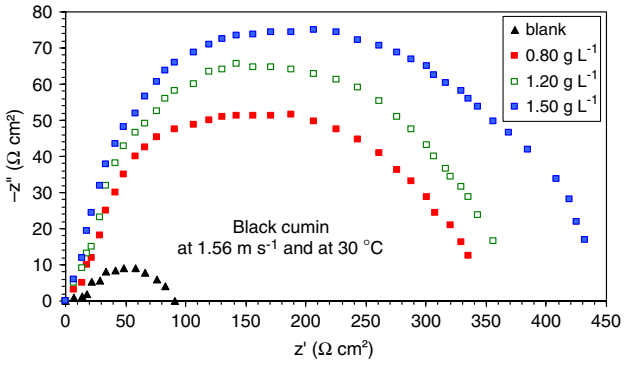

Fig. 7 Nyquist plots for low-carbon steel in industrial water in the absence and presence of various concentrations of black cumin at 30 °C and at 1.56 m s^{-1}

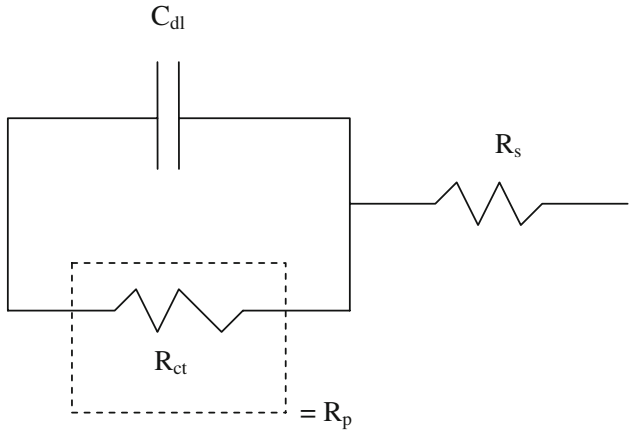

Fig. 8 The equivalent circuit model of the impedance spectroscopy

Table 4 Impedance parameters and the corresponding inhibition efficiency for low-carbon steel in industrial water in the absence and presence of radish leaves and black cumin at 30 °C and 1.56 m s^{-1}

Plants	C, g L^{-1}	R_{ct}, Ω cm^2	f_{max}, Hz	C_{dl}, µF	IE, %
	Blank	98.00	10.71	151.67	
Radish leaves	2.50	318.39	8.58	58.85	69.22
	3.88	377.50	8.58	49.14	74.04
Black cumin	1.20	351.00	8.58	52.85	72.08
	1.50	457.52	8.58	40.54	78.58

Table 3 Activation parameters and pre-exponential factor for low-carbon steel in industrial water in absence and presence of various concentrations of radish leaves and black cumin at 1.56 m s^{-1}

Plant	C, g L^{-1}	A, µA cm^{-2}	E_a, kJ mol^{-1}	ΔH_a, kJ mol^{-1}	$\Delta H_a = E_a - TR$, kJ mol^{-1}	ΔS_a, J mol^{-1} K^{-1}
	Blank	36,975	15.20	12.47	12.68	−166.58
Radish leaves	2.50	33,557	15.29	12.58	12.78	−167.38
	3.88	46,166	16.77	14.05	14.25	−168.65
Black cumin	1.20	27,134	17.74	15.30	15.22	−169.06
	1.50	25,109	18.07	15.56	15.55	−169.32

In this work, a maximum inhibition efficiency of radish leaves and black cumin on low-carbon steel in industrial water media at optimal temperature and velocity were at 3.88 and 1.50 g L^{-1}, respectively. A maximum performance of black cumin on low-carbon steel in industrial water was 77.59% (1.50 g L^{-1}) compared with 90.50% (1.14 g L^{-1}) of its inhibition efficiency on mild steel in acidic media (Ref 1).

3.3 Adsorption Isotherm

To investigate the mode of behavior of these compounds on the low-carbon steel surface in industrial water, the adsorption isotherm has been tested with several models such as Langmuir, Frumkin, Tumkin, Freundlich, Redlich-Peterson, and Flory-Huggins isotherms. The Flory-Huggins adsorption isotherm was found to be the best one for a description of this process. To obtain the isotherm, the fractional coverage values (Θ) as a function of inhibitor concentration was computed. The fraction coverage values can be calculated as follows (Ref 17, 18):

– weight loss measurements:

$$\Theta = \frac{W_a - W_p}{W_a} \quad \text{(Eq 7)}$$

where W_a and W_p are the CR of low-carbon steel in industrial water in the absence and presence of the inhibitors, respectively.

– polarization measurements

$$\Theta = \frac{I_{corr(a)} - I_{corr(p)}}{I_{corr(a)}} \quad \text{(Eq 8)}$$

where $I_{corr(a)}$ and $I_{corr(p)}$ are the corrosion current densities in the absence and presence of the inhibitors, respectively.

– impedance measurements

$$\Theta = \frac{(1/R_{ct})_a - (1/R_{ct})_p}{(1/R_{ct})_a} \quad \text{(Eq 9)}$$

where $R_{ct(a)}$ and $R_{ct(p)}$ are the charge transfer resistance in the absence and presence of the inhibitors, respectively.

According to Flory-Huggins model, Θ is related to the inhibitor concentration via:

$$\Theta/[x(1-\Theta)^x] = K_{ads}C \quad \text{(Nonlinear form)} \quad \text{(Eq 10)}$$

$$\log(\Theta/C) = \log K_{ads} + \log x + x\log(1-\Theta) \quad \text{(Linear form)} \quad \text{(Eq 11)}$$

where C is the inhibitor concentration (g L^{-1}), K_{ads} is the adsorption constant of the process (L g^{-1}), and x is the size parameter and is a measure of the number of adsorbed water molecules substituted by a given inhibitor molecules. The plot of log $(1-\Theta)$ versus log (Θ/C) gave straight lines as shown in Fig. 9(a) and (b) at 30 and 80 °C, respectively. The adsorption constant is related to the standard Gibbs free energy of adsorption, ΔG_{ads}, as follows (Ref 19):

$$K_{ads} = \frac{1}{1000}\exp\left(\frac{-\Delta G_{ads}}{RT}\right) \quad \text{(Eq 12)}$$

Here 1000 is the concentration of water in solution (g L^{-1}). This number was taken depending on the concentration of the inhibitor used, i.e., if the concentration is in mol L^{-1}, the above constant will be 55.5 (mol L^{-1}). From Table 5, it is evident that $(\partial G_{ads}/\partial t)_{T,P} < 0$) indicating that the Gibbs function was decreasing, predicting the spontaneity of the adsorption processes and stability of the adsorbed layer on the low-carbon steel surface. Moreover, the higher absolute values of ΔG_{ads} for black cumin indicate that it is more strongly adsorbed on the metal surface in industrial water. This is in good agreement with the range of the inhibition efficiency obtained from mass loss and potentiodynamic measurements (Table 1 and 2). This isotherm indicated a more actual adsorption by a molecule that has molecule quantity larger (Ref 20, 21) than Langmuir isotherm. The value of x is about 1.5, suggesting that one black cumin molecule can replace one and half water molecule-iron atom adsorptions when it adsorbed on the low-carbon steel surface

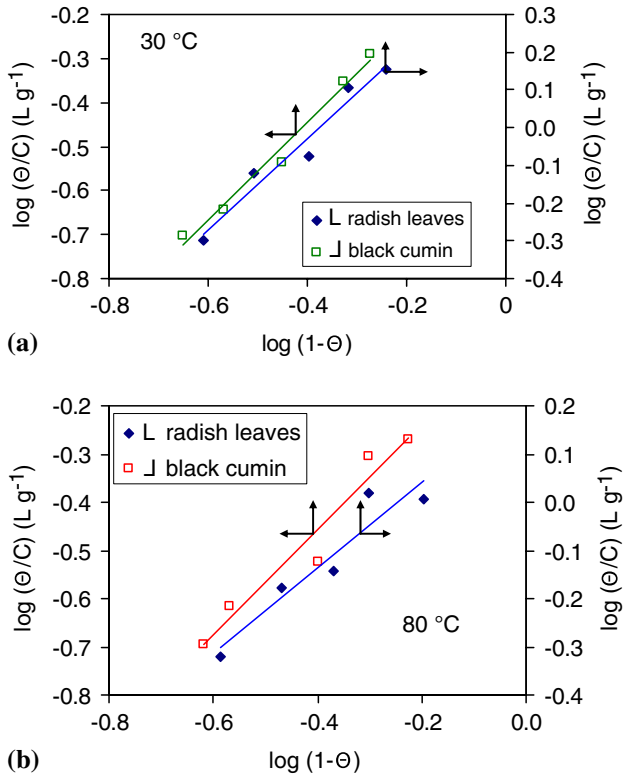

Fig. 9 Flory-Huggins adsorption isotherm model on the low-carbon steel surface in the presence of radish leaves and black cumin extracts at 30 °C (a) and 80 °C (b) and at 1.56 m s^{-1}

It is well known that the values of $(-\Delta G_{ads})$ of the order of 20 kJ mol^{-1} or lower indicate physisorption; those of order of 40 kJ mol^{-1} or higher involve charge sharing or a transfer from the inhibitor molecules to the metal surface to form a coordinate type of bond (Ref 22, 23). Therefore, the values of ΔG_{ads} obtained here indicate that, the adsorption mechanism of radish leaves and black cumin on low-carbon steel in industrial water is physisorption. Further, the enthalpy of adsorption (ΔH_{ads}) and entropy of adsorption (ΔS_{ads}) can be calculated via (Ref 24, 25):

$$\Delta H_{ads} = R\left(\frac{T_2T_1}{T_2 - T_1}\right)\ln\frac{k_2}{k_1} \quad \text{(Eq 13)}$$

$$\Delta S_{ads} = \frac{\Delta H_{ads} - \Delta G_{ads}}{T} \quad \text{(Eq 14)}$$

Additionally, the values of ΔH_{ads} and ΔS_{ads} can also be calculated using the following equation:

$$\ln K_{ads} = \ln\left(\frac{1}{1000}\right) - \frac{\Delta H_{ads}}{RT} + \frac{\Delta S_{ads}}{R} \quad \text{(Eq 15)}$$

Figure 10 shows the plot of ln K_{ads} versus $1/T$ which gives straight line with slope of $(-\Delta H_{ads}/R)$ and an intercept of $(\Delta S_{ads}/R - \ln 1000)$. The thermodynamic parameters are compiled in Table 5. The values of ΔH_{ads} obtained are in excellent agreement with those obtained from Eq 13, confirming the exothermic behavior of the adsorption of the studied plant extracts on the low-carbon steel surface in industrial water. The values of ΔS_{ads} are very close to each other indicating that the reactant complex on low-carbon steel in industrial water is stable.

3.4 Effect of Fluid Velocity

The experiment was carried out at various rotational speeds of the specimens in industrial water. As the fluid flows through the pipe, the rotational speed of the specimen is converted into flow rate of the fluid using the following empirical equations (Ref 26):

$$q = 0.92 n D_a^3 \left(\frac{D_t}{D_a}\right) \quad \text{(Eq 16)}$$

$$A_p = \pi D_a W \quad \text{(Eq 17)}$$

where q is the total flow rate from the edges of impeller ($m^3\ s^{-1}$), n is the number of rotations per second, D_a is the impeller diameter (m), D_t is the diameter of solution vessel (m), A_p is taken to be area of the cylinder swept out by the tips of the impeller blades (m^2), and W is the width of blades (m). The velocity of the fluid flow can be obtained from dividing Eq 16 by Eq 17. Tables 1 and 2 show that the IE (%) of black cumin and radish leaves was a maximum at 1.56 m s^{-1}. This is due to the fact that, at 1.56 m s^{-1}, the distribution of inhibitors is appropriate and the diffusion of dissolved oxygen might also encounter more difficulty to reach the metal surface because of the existence of the laminar layer. At all velocities, the inhibition efficiency of black cumin is relatively more than that of the radish leaves. IE (%) then began decreasing beyond 1.56 m s^{-1} because of impingement attack which is caused by the turbulent flow of solution over a metal surface. This is attributed to the fact that, at higher velocity, the extraneous impurities such as sand, dust, and scales, etc., embedded on the metal surface, cause pitting or scratching of the molecules of the absorbed layer and removes the adsorbed film away from the metal surface. Also, the mechanical effects act by breaking down the adsorbed layer. At this velocity, the flow is turbulent ($N_{Re} > 2100$); thereby the thinner laminar layer along the metal surface is reduced at higher velocity, leading to the dissolved oxygen easily reaching the metal surface causing more corrosion. Some changes in the entropy, enthalpy, and activation energy of the processes were noticed at different velocities. Experimentally it was found that the entropy of activation on low-carbon steel in industrial water in the presence of black cumin are −169.32 J mol^{-1} K^{-1} at 1.56 m s^{-1} and −158.47 J mol^{-1} K^{-1} at 1.44 m s^{-1} at 303 K and at optimum concentration. Thus, 1.56 m s^{-1} is the optimal velocity for studied inhibitors.

The relatively high inhibition efficiency obtained with black cumin (Fig. 3, Table 1, 2) rather than radish leaves may be attributed to the presence of cumaldehyde, fat oil, pentosan, and flavonoids (Ref 27) which enhance the film formation over the metal surface.

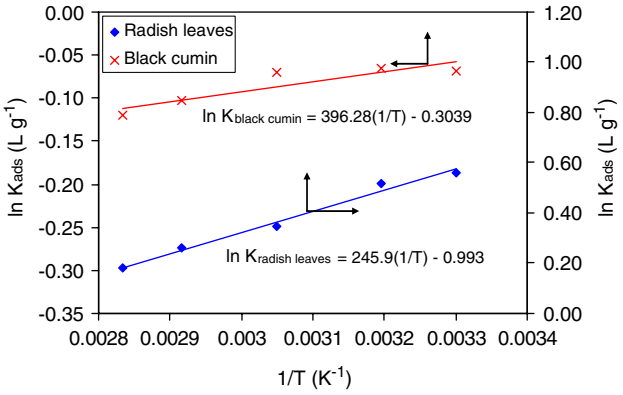

Fig. 10 Plot of ln K_{ads} vs. $1/T$

4. Conclusions

Black cumin and radish leaves are efficient, friendly, and low-cost inhibitors for low-carbon steel in industrial water. Optimization of temperature, inhibitor's concentration, and fluid velocity has been made. The IE (%) of black cumin and

Table 5 Thermodynamic parameters for adsorptions of radish leaves and black cumin on low-carbon steel in industrial water at different temperatures and at 1.56 m s^{-1}

Plant	T, K	x, L g^{-1}	K_{ads}, L g^{-1}	R^2	ΔG_{ads}, kJ mol^{-1}	ΔH_{ads}, kJ mol^{-1}	ΔS_{ads}, J mol^{-1} K^{-1}
Radish leaves	303	1.038	0.830	0.96	−16.93	...	...
	313	1.063	0.820	0.96	−17.46	−2.042(a)	49.18(a)
	328	0.847	0.780	0.87	−18.16	−2.045(b)	49.18(b)
	343	0.871	0.760	0.88	−18.92	...	...
	353	0.886	0.743	0.91	−19.40	...	...
Black cumin	303	1.101	2.630	0.98	−19.84	...	...
	313	1.466	2.657	0.91	−20.52	−3.180(a)	55.26(b)
	328	1.298	2.613	0.98	−21.46	−3.295(b)	55.40(a)
	343	1.151	2.333	0.97	−22.12	...	...
	353	1.095	2.200	0.95	−22.59	...	...

(a) Values obtained from Eq 13 and 14. (b) Values obtained from Eq 15

radish leaves increased with increasing concentration leading to increase of apparent activation energy and enthalpy of activation for the corrosion process. The adsorption of the studied inhibitors is well described by the Flory-Huggins isotherm model. Thermodynamic adsorption parameters indicated that the adsorption of black cumin and radish leaves on low-carbon steel surface in industrial water is physisorption. The data obtained reveal that the black cumin is relatively a better inhibitor than radish leaves.

Radish leaves and black cumin are advised to be used as good protective inhibitors, particularly in low-carbon steel pipes used for carrying oil and gas that contain a high content of water. They are nontoxic, low cost, and environment friendly. Furthermore, they can be used in the protection of heat exchangers, boilers tubes, and refinery units against aggressive normal and industrial water used for cooling or heating the equipments and products in industrial processes.

Acknowledgments

One of the authors (A. M. Badiea) is thankful to Mr. Nasr Humaidy, deputy of PEPA and Dr. Ahmed Abdillah, Chairman of PEPA (Ministry of Oil, Yemen) for providing some financial support and to Ms. Marry (Düsseldorf, Germany) for her help.

References

1. A.M. Abdel-Gaber, B.A. Abd-El-Nabey, I.M. Sidahmed, A.M. El-Zayady, and M. Saadawy, Inhibitive Action of Some Plant Extracts on the Corrosion of Steel in Acidic Media, *Corros. Sci.*, 2006, **48**, p 2765–2779
2. R.M. Saleh, A.A. Ismail, and A.A. El-Hosary, Corrosion Inhibition by Naturally Occurring Substances. VII. The Effect of Aqueous Extracts of Some Leaves and Fruit Peels on the Corrosion of Steel, Aluminum, Zinc and Copper in Acids, *Br. Corros. J.*, 1982, **17**, p 131–135
3. K. Srivatsava and P. Srivatsava, Studies on Plant Materials as Corrosion Inhibitors, *Br. Corros. J.*, 1981, **16**, p 221–223
4. A.Y. El-Etre, Natural Honey as Corrosion Inhibitor for Metals and Alloys. I. Copper in Neutral Aqueous Solution, *Corros. Sci.*, 1998, **40**, p 1845–1850
5. A.Y. El-Etre and M. Abdallah, Natural Honey as Corrosion Inhibitor for Metals and Alloys. II. C Steel in High Saline Water, *Corros. Sci.*, 2000, **42**, p 731–738
6. E. Khamis and N. Al-Andis, Herbs as New Type of Green Inhibitors for Acidic Corrosion of Steel, *Materwiss. Werkstofftech.*, 2002, **33**, p 550–554
7. A. Chetouani and B. Hammouti, Corrosion Inhibition of Iron in Hydrochloric Acid Solutions by Naturally Henna, *Bull. Electrochem.*, 2003, **19**, p 23–25
8. B. Hammouti, S. Kertit, and M. Melhaoui, Bgugaine: A Natural Pyrolidine Alkaloid Product as Corrosion Inhibitor of Iron in HCl Medium, *Bull. Electrochem.*, 1995, **11**, p 553–555
9. B. Hammouti, S. Kertit, and M. Melhaoui, Electrochemical Behaviour of Gugaine as Corrosion Inhibitor of Iron in HCl Medium, *Bull. Electrochem.*, 1997, **13**, p 97–98
10. M.K. Gomma and M.H. Wahdan, Schiff Bases as Corrosion Inhibitors for Aluminum in Hydrochloric Acid Solution, *Mater. Chem. Phys.*, 1995, **39**, p 209–213
11. M.G. Fontana and N.D. Green, *Corrosion Engineering*, 2ndMcGraw-Hill, New York, 1978
12. M.A. Ameer, E. Khamis, and G. Al-Senani, Effect of Temperature on Stability of Adsorbed Inhibitors on Steel in Phosphoric Acid Solution, *J. Appl. Electrochem.*, 2002, **32**, p 149–156
13. B.A. Abd-El-Nabey, E. Khamis, M.Sh. Ramadan, and A. El-Gindy, Application of the Kinetic-Thermodynamic Model for Inhibition of Acid Corrosion of Steel by Inhibitors Containing Sulfur and Nitrogen, *Corrosion*, 1996, **52**, p 671–679
14. N.H. Helal, M.M. El-Rabiee, Gh.M. Abd El-Hafez, and W.A. Badawy, Environmentally Safe Corrosion Inhibition of Pb in Aqueous Solutions, *J. Alloys Compd.*, 2008, **456**, p 372–379
15. J. Cruz, R. Martínez, J. Genesca, and E. García-Ochoa, Experimental and Theoretical Study of 1-(2-Ethylamino)-2-methylimidazoline as an Inhibitor of Carbon Steel Corrosion in Acid Media, *J. Electroanal. Chem.*, 2004, **566**, p 111–121
16. M. Hosseini, S.F.L. Mertens, M. Ghorbani, and M.R. Arshadi, Asymmetrical Schiff Bases as Inhibitors of Mild Steel Corrosion in Sulphuric Acid Media, *Mater. Chem. Phys.*, 2003, **78**, p 800–808
17. O. Benali, L. Larabi, M. Traisnel, L. Gengembre, and Y. Harek, Electrochemical, Theoretical and XPS Studies of 2-Mercapto-1-methylimidazole Adsorption on Carbon Steel in 1 M $HClO_4$, *Appl. Surf. Sci.*, 2007, **253**, p 6130–6139
18. F. Bentiss, M. Lagrené, M. Traisnel, and J.C. Hornez, Corrosion Inhibition of Mild Steel in 1 M Hydrochloric Acid by 2,5-Bis(2-Aminophenyl)-1,3,4-Oxadiazole, *Corrosion*, 1999, **55**, p 968–976
19. T.F. Tadros, *Applied Surfactants*, Wiley-VCH, Weinheim, 2005, p 87
20. E.E. Oguzie, C. Unaegbu, C.N. Ogukwe, B.N. Okolue, and A.I. Onuchukwu, Inhibition of Mild Steel Corrosion in Sulphuric Acid Using Indigo Dye and Synergistic Halide Additives, *Mater. Chem. Phys.*, 2004, **84**, p 363–368
21. S.S. Abd El Rehim, M.A.M. Ibrahim, and K.F. Khalid, The Inhibition of 4-(2′-Amino-5′-methylphenylazo) antipyrine on Corrosion of Mild Steel in HCl Solution, *Mater. Chem. Phys.*, 2001, **70**, p 268–273
22. F.M. Donahue and K. Nobe, Theory of Organic Corrosion Inhibitors: Adsorption and Linear Free Energy Relationships, *J. Electrochem. Soc.*, 1965, **112**, p 886–891
23. E. Khamis, F. Bellucci, R.M. Latanision, and E.S.H. El-Ashry, Acid Corrosion Inhibition of Nickel by 2-(Triphenosphoranylidene) Succinic Anhydride, *Corrosion*, 1991, **47**, p 677–686
24. M. Soleimani and T. Kaghazchi, The Investigation of the Potential of Activated Hard Shell of Apricot Stones as Gold Adsorbents, *J. Ind. Eng. Chem.*, 2008, **14**, p 28–37
25. U. Inel, D. Topalogln, A. Askin, and F. Tumsek, Evaluation of the Thermodynamic Parameters for the Adsorption of Some Hydrocarbons on 4A and 13X Zeolites by Inverse Gas Chromatography, *Chem. Eng. J.*, 2002, **88**, p 255–262
26. L. Warren, C.S. Julian, and P. Hariott, *Unit Operations of Chemical Engineering*, 4th ed., McGraw Hill, New York, 1985, p 217–219, 690
27. H. Armoosh, *The Herbs in Book*, 1stHouse of the Gems, Damascus, 1999